Appl Magn Reson (2017) 48:687–698
DOI 10.1007/s00723-017-0909-6

Applied Magnetic Resonance

ORIGINAL PAPER

Reduction of Effect of Concomitant Gradients in Low Magnetic Field MRI via Optimization of Gradient Magnetic System

Vladimir Chizhik[1] · Vyacheslav Frolov[1] · Pavel Kupryanov[1] · Konstantin Tyutyukin[1]

Received: 31 January 2017 / Revised: 13 May 2017 / Published online: 17 June 2017

Abstract The effect of concomitant magnetic fields emerging in conjunction with encoding gradients, which is important in the process of the magnetic resonance imaging in low fields, has been considered. The manifestations of concomitant magnetic fields in a concrete gradient system, namely in the system of two coaxial gradient coils, have been thoroughly analyzed. It has been suggested to improve the gradient system via optimization of the interspace between coils on the basis of the standard criterion of the minimum of root-mean-square deviation of the encoding field dependence from a linear one. It has been shown that the optimal interspace is not the Maxwell condition.

1 Introduction

As a rule, the routine studies in the area of magnetic resonance imaging (MRI) are carried out in high magnetic fields (several Tesla), that ensures a good signal/noise ratio and, therefore, a small examination time. However, the increase in the magnitude of a static magnetic field (and, hence, in the resonance frequency) is associated not only with positive factors: (a) the radiofrequency power is more absorbed at high frequencies due to the electric conductance of organism tissues, which results in degradation of signal/noise ratio [1]; (b) because of the effect of relaxation rate dispersion, in high fields, the decrease in the MRI-contrast for T_1- and T_2-weighted images takes place [2]; (c) there are procedure difficulties for certain patient groups (it is impossible to examine patients with metallic implants, cardiac pacemakers, etc., persons suffering with claustrophobia; some patients cannot stand the noise produced by gradient-switching systems) [3]. Nevertheless, a

✉ Vyacheslav Frolov
vfrolovv@bk.ru

[1] Faculty of Physics, Saint Petersburg State University, Saint-Peterburg, Russia

number of medical diagnostic and technological problems can be solved in low magnetic fields, including the Earth's magnetic field [4, 5].

The first detection of NMR in the Earth's magnetic field (EFNMR) was carried out in the early 50s [6], but for a long time, the EFNMR method was mainly used in the area of magnetometry. Up to the recent time, EFNMR was realized outdoors, where the level of external hindrances was very low and there was no disturbance of the homogeneity of a static magnetic field. Now, a few successful realizations of EFNMR in laboratory conditions have been described (see [5, 7]). The first publications on MRI in the Earth's magnetic field (EFMRI) appeared in the 80s [8–12]. The following development of EFMRI is reflected, for example, in the works [13, 14]. The low price and high mobility of equipment attracted the additional attention to the EFMRI [15]. It is worth noting that MRI in low fields was used for the visualization of polarized gases [16] that is applicable for the lung imaging. The low field MRI is used not only in medicine, but also in oil and water geophysics, in chemical technologies [17, 18], and it can be perspective for the control of liquid explosives, theirs precursors, and other illicit and hazardous compounds [4, 7]. Therefore, the magnetic resonance imaging in low fields [19], in particular such as Earth's field [20, 21] or less ones (microtesla NMR with hyperpolarization and SQUID registration [22]), becomes the widespread subject of studies.

For the realization of the MRI method, it is necessary to create accurately linear magnetic field gradients (MFG) extending over rather big volumes (up to 0.1 m^3). Despite of the crucial role MFG in MRI, the surprising small number of works made major contribution to the elaboration of the problem. There were few attempts to optimize the design of gradient systems (they were partly reviewed in [23]).

In the aspect of the quality of MRI in low fields, it is useful to consider the effect of additional, named "concomitant", fields which arise in gradient systems. It is known that according to the Maxwell equations, the appearance of a gradient of the certain component of a potential field unavoidably causes gradients of other (orthogonal) field components. The static magnetic field is potential, and hence, this effect must manifest in the procedure of getting NMR images (see [24]). To determine the position of a volume element (voxel) or, in other words, to execute a spatial encoding, an additional magnetic field with a spatially homogeneous constant gradient is applied along the chosen coordinate axes. It is usually supposed that in this way, the direct proportionality of the NMR frequency to a coordinate is attained. Nevertheless, if one takes into account concomitant gradients, the additional magnetic field components in orthogonal directions are shown up [25] and the required proportionality is violated. As a result, the concomitant gradients cause both an error in the mapping of a voxel position and distortion of the spatial distribution of signal intensity. The effect is negligible for the routine MRI in high fields; however, it can be very important in low field MRI experiments [13, 26–28]. Here, we consider the problem in detail and propose a method to minimize the distortion of the "longitudinal" gradient (along the main field) by undesirable "transversal" gradients.

2 Preliminary Remarks

To produce the spatial encoding of NMR signals, the spatially homogeneous gradients of a static magnetic field are used. Components of a magnetic field **B** obey the Maxwell equations which in current-free space take the form

$$\text{rot } \mathbf{B} = 0,$$
$$\text{div } \mathbf{B} = 0.$$

From the first equation, it follows:

$$\frac{\partial B_\mu}{\partial x_\nu} = \frac{\partial B_\nu}{\partial x_{\mu_\mu}}$$

(x_μ denotes x, y, and z) and from the second one:

$$\frac{\partial B_z}{\partial z} + \frac{\partial B_x}{\partial x} + \frac{\partial B_y}{\partial y} = 0.$$

Therefore, the appearance of any derivative inevitably leads to the existence of at least another one. The appearance of transversal components is visually demonstrated with Fig. 1 where field lines of the additional field $\mathbf{B}_\mathrm{G}$ with a longitudinal gradient $G_z = \frac{\partial B_{Gz}}{\partial z}$ (along z) are represented. The existence of the z-component of a gradient **G** is reflected by an increasing of the density of the field lines. Since in the presence of some gradient field, lines cannot be parallel, an orthogonal x-component $B_{\mathrm{G}x}$ appears.

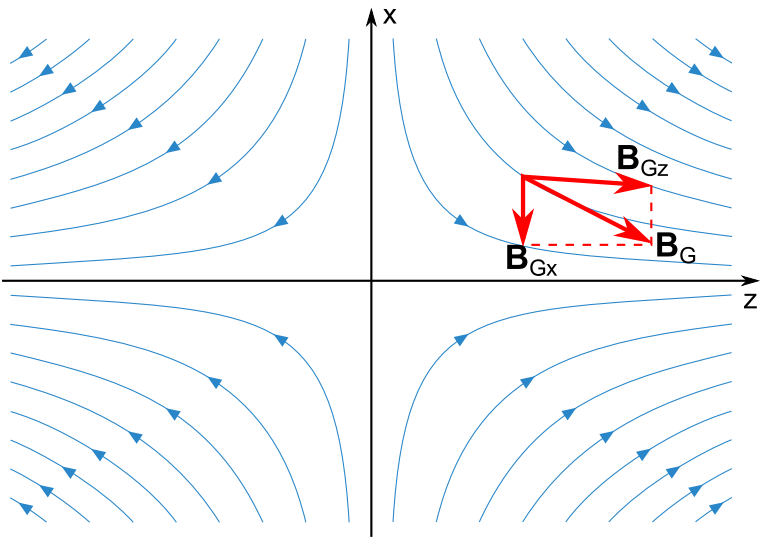

Fig. 1 Field lines of the field $\mathbf{B}_\mathrm{G}$ with a gradient G_z and the vector diagram, which reveals the appearance of the x-component of $\mathbf{B}_\mathrm{G}$

The total field $\mathbf{B}_{\text{tot}}$ is the vector sum of a «main» (homogeneous) field $\mathbf{B}_0$ (along z) and a field produced by gradient system $\mathbf{B}_{\text{G}}$. In the case of the longitudinal gradient G_z

$$B_{\text{tot}} = \left[(B_0 + G_z z)^2 + \left(x \frac{\partial B_x}{\partial x} \right)^2 + \left(y \frac{\partial B_y}{\partial y} \right)^2 \right]^{1/2}. \quad (1)$$

Here, G_z is the gradient, which is routinely used to obtain an image, and B_x and B_y are the concomitant field components. As a result, the NMR frequency is not directly proportional to the z-coordinate but depends on the module of the total field $|\mathbf{B}_{\text{tot}}|$.

It follows from Eq. (1) that the encoding field is $B_{\text{encod}} = B_{\text{tot}} - B_0$ (instead of $B_{\text{encod}} = G_z z$), and it is not linear with respect to the z-coordinate. Thus, the existence of concomitant magnetic fields leads to distortions of the mapping of voxel spatial position, especially in remote from the origin elements of an investigated object. The less the main magnetic field B_0 is, the more the effect of concomitant gradients is important. Here, we propose and describe, in detail, a simple method to minimize this harmful effect on the example of a concrete gradient system.

The basic design of an axial gradient system is the pair of coils (with oppositely directed currents) of a radius R which are separated by a distance $L = \sqrt{3}R$ (the Maxwell condition). Let the field $\mathbf{B}_0$ is directed along the z-axis (see Fig. 2) of the polar coordinate system (z, ρ, φ). The realization of the Maxwell condition provides the equality to zero of the third derivative of the z-component of the magnetic field

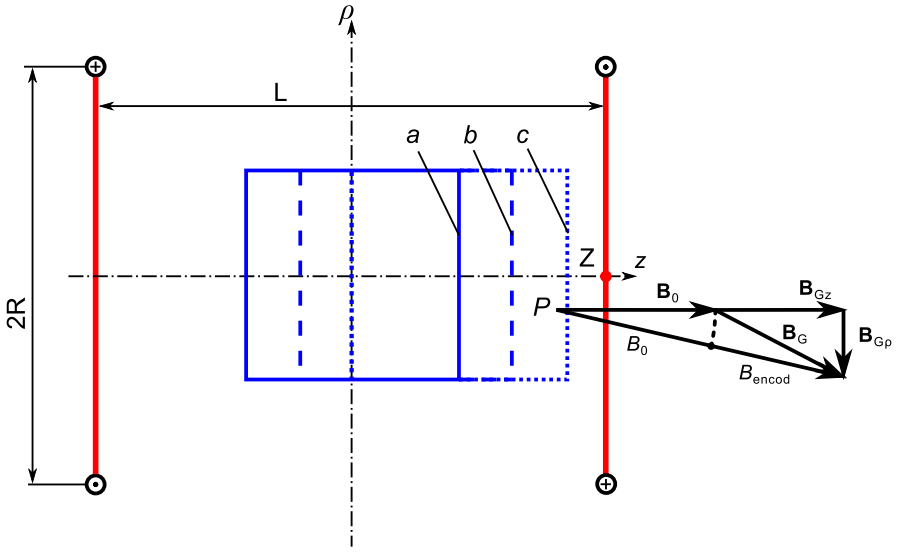

Fig. 2 Cross-sectional drawing of an axial gradient system consisting of two coils. Three positions of an object under study: symmetric (*a*), half-shifted (*b*), completely shifted to positive z (*c*) are shown. The formation of the encoding field B_{encod} for point P as the difference between B_{tot} and B_0 is also demonstrated

$\mathbf{B}_G$ on z at the system isocentre ($z = 0$, $\rho = 0$) that allows one to obtain the best field linearity, but only near the coordinate origin. It is also obvious from Eq. (1) that the concomitant gradients do not create any additive fields on the axis z ($x = y = 0$ or $\rho = 0$). However, voxels, which are out of the z-axis, form the basic area of an image. The NMR frequency for an every voxel is determined by the total field module according to Eq. (1), and the Maxwell condition is not optimum to get the best linearity of the encoding field over the whole object volume. We propose a simple option to minimize the undesirable effect of concomitant gradients via the change of interspace-to-diameter ratio for coils that can allow one to optimally use the "working volume" of a tomograph.

3 Basic Relations. Maxwell Gradient System

The calculations of magnetic field components in polar coordinates (z, ρ, φ) were carried out using the well-known integral formulas based on the Biot–Savart–Laplace law [29, 30]:

$$B_{Gz} = \frac{1}{\pi}\int_0^{\pi}(1-\rho\cos\varphi) \times \left[\frac{1}{\left[1+(z-Z)^2+\rho^2+2\rho\cos\varphi\right]^{3/2}} - \frac{1}{\left[1+(z+Z)^2+\rho^2+2\rho\cos\varphi\right]^{3/2}}\right]\mathrm{d}\varphi, \tag{2}$$

$$B_{G\rho} = \frac{z-Z}{\pi}\int_0^{\pi}\frac{\cos\varphi\mathrm{d}\varphi}{\left[1+(z-Z)^2+\rho^2+2\cos\varphi\right]^{3/2}} - \frac{z+Z}{\pi}\int_0^{\pi}\frac{\cos\varphi\mathrm{d}\varphi}{\left[1+(z+Z)^2+\rho^2+2\rho\cos\varphi\right]^{3/2}}. \tag{3}$$

Here, B_{Gz} and $B_{G\rho}$ are the axial and radial components of the magnetic field of the gradient system, respectively. In Eqs. (2) and (3) and below, the dimensionless units are used for both distances and fields: all distances are measured in units of the coil radius R and magnetic fields are expressed in units of $\mu_0 In/2R$, where μ_0 is the magnetic constant ($4\pi \times 10^{-7}$ Ω s/m); I is the electric current in the coils (a filamentary current approximation is supposed); n is the number of turns. The numeric computations and graphics were performed using MathCad® 15.

As it follows from the above, the manifestation of the concomitant field effect depends on (a) the relation between the size of an object to be investigated and the dimensions of a gradient system, and (b) the object position in a gradient system. Herewith, the system design must provide the maximal workspace of a tomograph with the admissible nonlinearity of the encoding field B_{encod}. In the case of axially

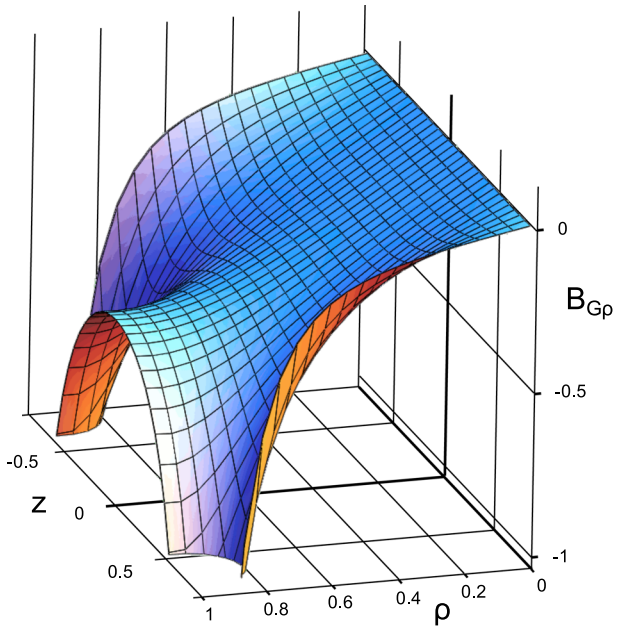

Fig. 3 Relief diagram of the ρ-component of the Maxwell gradient system field

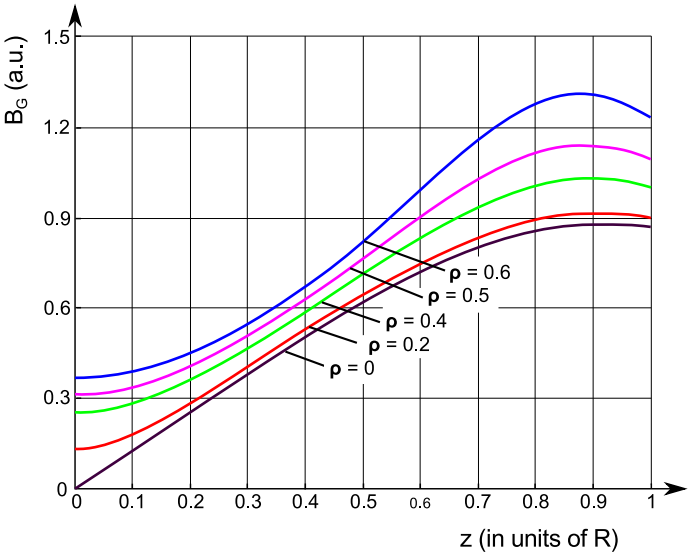

Fig. 4 Dependences of the field B_G (produced by Maxwell gradient system) on z for different distances from axis (ρ)

symmetric systems, namely the radial component of the total field, $B_{G\rho}$, takes on the role of a concomitant field and determines the nonlinearity of the encoding field. In Fig. 3, the dependence of $B_{G\rho}$ on z and ρ in the Maxwell gradient system is shown.

Figure 4 represents the field B_G dependence on z for different ρ, and it is important that the marked increase in the nonlinearity occurs for big ρ at small z-values where z-component is most linear. The effect is explained by the fact that the encoding field in this zone is determined mainly by the ρ-component. For z-values close to $\pm L/2$, the main cause of the encoding field nonlinearity is the own behavior of the z-component (see the comments to the Maxwell condition).

To realize MRI, the combination of a homogeneous ("main") field and a field of a gradient system is always used. It is convenient to introduce the parameter k which is determined as the ratio of the main field B_0 to the maximum field of a gradient system, B_{Gz}, in the limits of an investigated object:

$$k = B_0/B_{Gz\max}.$$

For definiteness, we have chosen the k value for the cylindrical object which the length and the diameter were equal to the coil radius R.

Figure 5 demonstrates the contribution of the Maxwell gradient system to the encoding field (B_{encod}) for different values k and distances from the axis ρ. In Fig. 5a, the dependences of B_{encod} on z for $\rho = 0.5$ are represented for different k. The similar dependences for different ρ values and for $k = 0.5$ and 2 are presented in Fig. 5b. It is evident that in Fig. 5a and b, the zone of negative z, where the B_0 and gradient field B_{Gz} are opposite is absolutely unfitted for the spatial encoding when $k \leq 1$. In that situation, it is reasonable to shift an investigated object to positive z.

4 Optimization of Gradient System. Results and Discussion

We suggest to improve the gradient system via the optimization of the coil interspace L on the basis of the standard criterion of the minimum root-mean-square deviation of the z-dependence of the encoding field from a linear one. The dependences of the encoding field on z-coordinate were obtained (analogously to

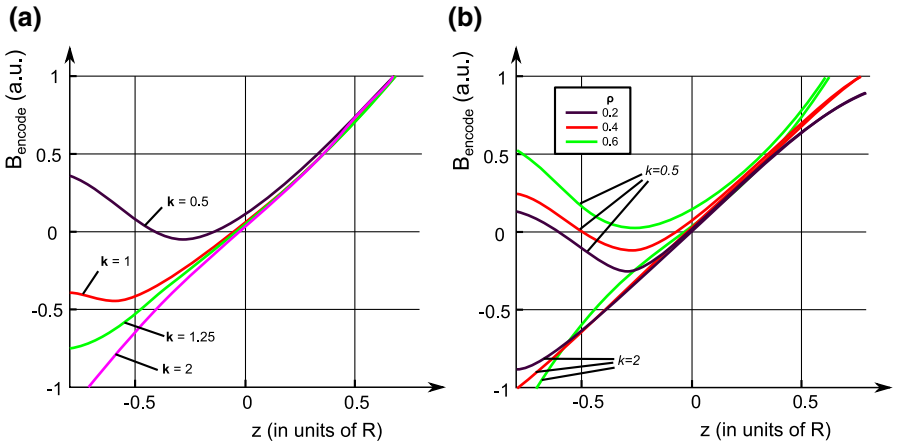

Fig. 5 Encoding field in the Maxwell system as a function of z for different main field values (k) at $\rho = 0.5$ (**a**) and for different distances (ρ) from the axis for $k = 0.5$ and 2 (**b**)

Fig. 5) for different interspaces between the coils. Then, the relative standard error (RSE) of the deviation of those dependencies from linear ones for various object positions was calculated. The linear dependences were obtained within Mathcad® using functions line(x,y), where $x = z$ and $y = B_{\text{encod}}$. The calculus of the Standard Error was made within Mathcad® function stderr(x,y). The relative standard error was obtained as the ratio of the standard error to the maximum field produced by gradient system, $(B_{\text{Gz}})_{\text{max}}$ in the limits of an investigated object. This maximum field is defined as the product of a slope of the calculated linear dependence into the half length of an object.

First, the calculations were carried out for the case of the above cylindrical object which the length and diameter were equal to the coil radius (see Fig. 2). The RSE dependences on the coil interspace L for different values of k in the case of the symmetric object disposition (a in Fig. 2) are represented in Fig. 6. One can see from Fig. 6a that the use of the Maxwell system results in the large RSE in the case, when a homogeneous field is comparable to a gradient system field ($k \leq 1$). To reduce RSE, it is possible to increase the coils interspace, but the disadvantage of this approach is the significant increase of a system dimension and the reduction of gradient system efficiency. For $k > 1$, it is possible to suggest the better solution, because the RSE dependences on the interspace have a minimum. This fact allows us to realize the minimum RSE by the moderate change of the interspace L (see Fig. 6b). To illustrate the latter, we present in Fig. 7 the relative deviation (not RSE!) of the field B_{encod} from linear dependence in the case of the symmetrical position of an investigated object (a in Fig. 2) for the optimal interspace and Maxwell condition and for two values of the main field ($k = 1.1$ and 10). Note: if the homogeneous (main) field is in ten times greater than the maximum gradient field in the limits of an object ($k = 10$), the interspace optimization reduces RSE in four times (in comparison with the case of the Maxwell condition).

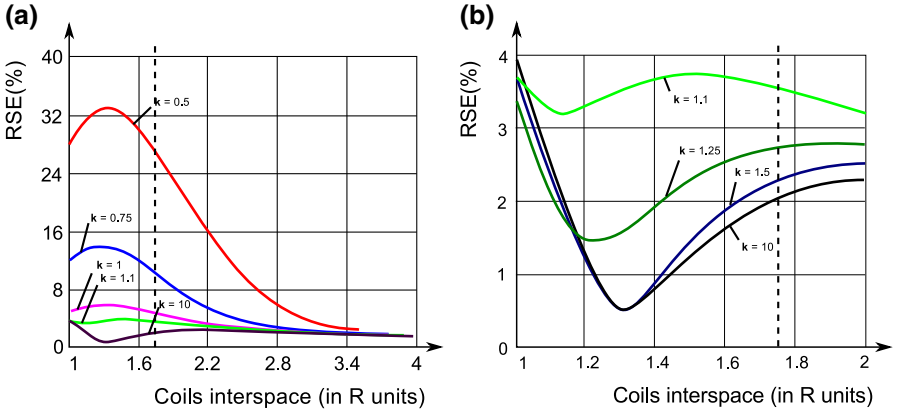

Fig. 6 Dependence of the relative standard error on the coil interspace L; in the case, the symmetrical object position for different values of the homogeneous field: **a** $k = 0.5$, 0.75, 1, 1.1, and 10; **b** in the larger scale $k = 1.1$, 1.25, 1.5, and 10. The *dotted line* indicates the Maxwell condition

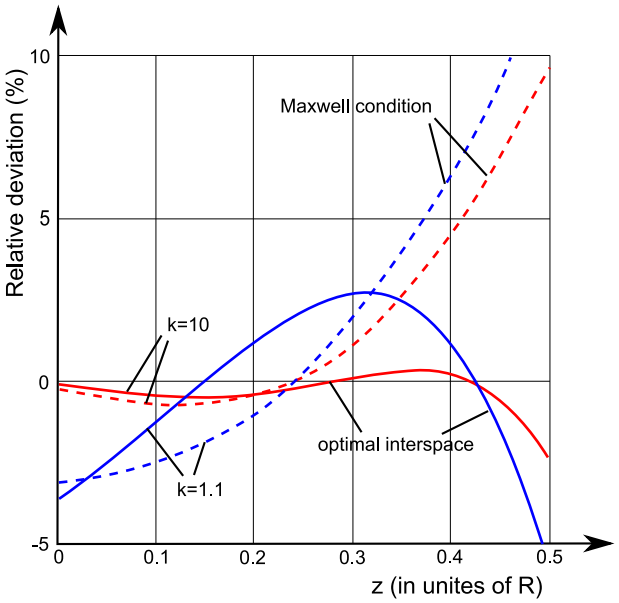

Fig. 7 Comparison of the relative deviation of the field B_{encod} from the linear dependence for the Maxwell condition and optimal interspace in the case of the symmetrical position of an investigated object (*a* in Fig. 2)

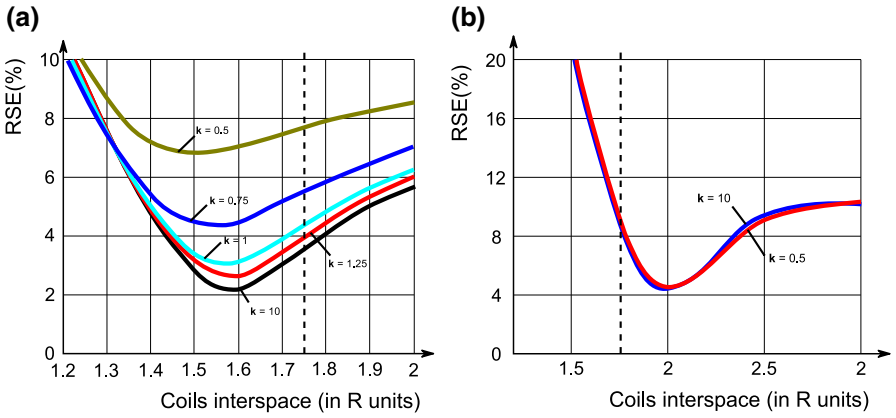

Fig. 8 Dependence of RSE on the coil interspace for the shifted object. **a** Object is shifted by half of the coil radius to the positive *z* (the position *b* in Fig. 2); **b** object is completely shifted to the positive *z* (the position *c* in Fig. 2). The *dotted line* indicates the Maxwell condition

In Fig. 8, the dependences of RSE on the coil interspace for an object shifted from the center of a gradient system (the position *b* and *c* in Fig. 2) are represented. Figures 6b and 8 demonstrate that it is possible to considerably improve the linearity of the field B_{encod} choosing the optimum coil interspace (without the increase in dimensions of a gradient system and with the better use of a work volume).

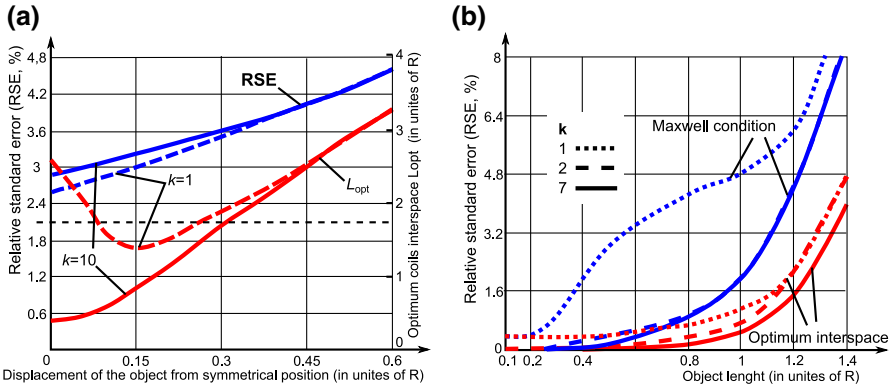

Fig. 9 Dependences of the optimal interspace L_{opt} and RSE on an object position (**a**); dependences of RSE for the optimum and Maxwell interspaces on an object dimensions (**b**) for the main field characterized by the values $k = 1, 2, 10$. See the text for the information on the length and diameter of an object

Figure 9 shows the computed dependences of the optimal interspace L_{opt} and RSE on the position (Fig. 9a) and on dimensions (Fig. 9b) of an object for different values of the main field. As above, an object is supposed of cylindrical form, and its diameter is equal to the coil radius *R,* and besides for Fig. 9a, the object length is equal its diameter. It can be seen that the shift of an object (in the direction of the main field) decreases the dependence on the main field, but RSE increases. Figure 9b demonstrates the absence of the optimum for $k = 1$, but the dependence of the optimal position on the main field quickly relaxes for $k > 1$ (the dependences for $k = 2$ and $k = 10$ are virtually indistinguishable).

5 Conclusion

In connection with the growing interest to the magnetic resonance imaging in low fields, it was important to consider in detail the effect of concomitant magnetic fields emerging in conjunction with encoding gradients. We investigated this effect, which distorts the quality of magnetic resonance images, in the case of the basic design of an axial gradient system—the pair of coils with oppositely directed currents (a particular case is the Maxwell gradient system). It has been suggested to improve the gradient system via the optimization of the interspace between coils on the basis of the standard criterion of the minimum root-mean-square deviation of the *z*-dependence of the encoding field from a linear one. In particular, if the maximum gradient field in the limits of an investigated object is less than the main homogeneous field ($k > 1$), the interspace L between the coils should be decremented in comparison with the Maxwell condition ($\sqrt{3}$) up to 1.2–1.4 for objects which dimensions are about the coil radius. In the case of low main fields ($k \leq 1$), it is expedient to increase strongly the interspace L (see Fig. 6a) and to shift an object in the direction of the main field (Fig. 8), but wherein the efficiency of a

gradient system is reduced (it is necessary to increase significantly the current in coils).

In conclusion, we present the estimations of the parameters of the experimental conditions for obtaining MR images in the Earth's magnetic field (50 μT, i.e., the proton resonance frequency is about 2100 Hz). The required encoding gradient is determined by the acceptable dimension of a pixel and NMR line width $\delta v = 1/(\pi T_2)$, where T_2 is the spin–spin relaxation time. The T_2 values for tissues lie within the range 50–300 ms [3]. Assuming that the spin–spin relaxation time of an investigated object is $T_2 = 100$ ms, one can conclude that the frequency difference between adjacent pixels should be of 3 Hz. If the object diameter and length are 25 cm (a human head) and the desirable spatial resolution (pixel dimension) is 2–3 mm, then the gradient characterized in the frequency scale will be about 300 Hz and the parameter $k = 7$. If the coil diameter is 50 cm (such a relation with the object dimensions was supposed in our study), from the graph of Fig. 6, we obtain $L = 1.3$, $R = 65$ cm, with RSE of 0.5% (for the Maxwell system, RSE is about 2%).

The diminution of the coil diameter on 20% gives the error in three times more but for the Maxwell distance—more than 10 times. However, its enlargement up to 1 m reduces RSE for the optimal interspace to a neglected value <0.01% and for the Maxwell distance—to 0.13%.

References

1. W. Edelstein, G. Glover, C. Hardy, R. Redington, Magn. Reson. Med. **3**, 604–618 (1986)
2. R.G. Bryant, D.A. Mendelson, C.C. Lester, Magn. Reson. Med. **21**, 117–126 (1991). doi:10.1002/mrm.1910210114
3. P.A. Rinck, *Magnetic Resonance in Medicine* (Blackwell Wissentshafts-Verlag, Berlin, Wien, 2001)
4. N.A. Krylatykh, Y.V. Fattakhov, A.R. Fakhrutdinov, V.N. Anashkin, V.A. Shagalov, R.S. Khabipov, Appl. Magn. Reson. **47**(8), 915–924 (2016)
5. M.E. Halse, A. Coy, R. Dykstra, C. Eccles, M. Hunter, R. Ward, P.T. Callaghan, J. Magn. Reson. **182**, 75–83 (2006)
6. M.E. Packard, R. Varian, Phys. Rev. **93**, 941 (1954)
7. E. Balcı, B. Rameev, H. Acar, G.V. Mozzhukhin, B. Aktas, B. Çolak, P.A. Kupriyanov, A.V. Ievlev, Y.S. Chernyshev, V.I. Chizhik, Appl. Magn. Reson. **47**(1), 87–99 (2016). doi:10.1007/s00723-015-0730-z
8. J. Stepišnik, in *Proceedings of the XXII Congress AMPERE* (Switzerland, Zürich, 1984) pp. 528–529
9. J. Stepišnik, D. Mihajlovic, in *Abstracts of the 7th Specialized Colloque AMPERE* (Romania, Bucharest, 1985) p. 194
10. H. Mehier, M. Maurice, J.P. Bonche, G. Jacquemod, C. Desuzinges, B. Favre, J.O. Peyrin, J. Biophys. Biomed. **9**, 198 (1985)
11. J. Stepišnik, V. Eržen, D. Mihailovic, in *Proceedings of the 8th European Experimental NMR Conference* (Belgium, Spa, 1986) p. 145
12. J. Stepišnik, V. Eržen, D. Mihailovic, B.B. Lavrenčič, A. Čadež, Farm. Vest. **37**, 135–137 (1986)
13. A. Mohorič, G. Planinšič, M. Kos, A. Duh, J. Stepišnik, Instrum. Sci. Technol. **32**, 655–667 (2004)
14. J. Stepišnik, V. Eržen, M. Kos, Magn. Reson. Med. **15**, 386–391 (1990)
15. D. Kleppner, Phys. Today **45**(7), 9–10 (1992)
16. C.H. Tseng, G.P. Wong, V.R. Pomeroy, R.W. Mair, D.P. Hinton, D. Hoffman, R.E. Stoner, F.W. Hersman, D.G. Cory, R.L. Walsworth, Phys. Rev. Lett. **81**, 3785–3788 (1998)

17. L.-S. Bouchard, S.R. Burt, M.S. Anwar, K.V. Kovtunov, I.V. Koptyug, A. Pines, Science **319**(5862), 442–445 (2008)
18. O.A. Shushakov, A.G. Maryasov, Appl. Magn. Reson. **47**, 1021–1032 (2016)
19. A.M. Coffey, M. Truong, E.Y. Chekmenev, J. Magn. Reson. **237**, 169–174 (2013)
20. G. Planinsic, J. Stepisnink, M. Kos, J. Magn. Reson. **A110**, 170–174 (1994)
21. A. Mohoric, G. Planinsic, M. Kos, A. Duh, J. Stepisnik, Instrum. Sci. Technol. **32**, 655 (2004)
22. R. McDermott, A.H. Trabesinger, M. Mueck, E.L. Hahn, A. Pines, J. Clarke, Science **295**, 2247–2249 (2002)
23. R. Turner, Magn. Reson. Imaging **11**, 903–920 (1993)
24. D.G. Norris, J.M.S. Hutchison, Magn. Reson. Imaging **8**, 33–37 (1990)
25. M.A. Bernstein, K.F. King, X.J. Zhou, *Handbook of MRI Pulse Sequences* (Elsevier, Oxford, 2004), pp. 292–305
26. X.J. Zhou, Y.P. Du, M.A. Bernstein, H.G. Reynolds, J.K. Maier, J.A. Polzin, Magn. Reson. Med. **39**, 596–605 (1998)
27. X.J. Zhou, S.G. Tan, M.A. Bernstein, Magn. Reson. Med. **40**, 582–591 (1998)
28. C.T. Sica, C.H. Meyer, Magn. Reson. Med. **57**(4), 721–730 (2007)
29. B.L. Alievskii, A.V. Oktiabrskii, V.I. Orlov, *The Calculation of the Axially Symmetric Coils Magnetic Field Parameters* (MAI, Moscow, 1999). **(in Russian)**
30. W.R. Smyte, *Static and Dynamic Electricity*, 3rd edn. (CRC Press, NY, 1989)